Modeling Surgical Loads to Account for Subsurface Tissue Deformation During Stereotactic Neurosurgery

Michael I. Miga*, Keith D. Paulsen*+#[0], Francis E. Kennedy*,
P. Jack Hoopes*+#, Alex Hartov*+, David W. Roberts+#

*Thayer School of Engineering, Dartmouth College, Hanover, N.H., 03755
+Dartmouth Hitchcock Medical Center, Lebanon, N.H., 03756
#Norris Cotton Cancer Center, Lebanon, N.H., 03756

ABSTRACT

For more than a decade, surgical procedures have benefited significantly from the advent of OR (operating room) coregistered preoperative CT (computed tomographic) and MR (magnetic resonance) imaging. Despite advances in imaging and image registration, one of the most challenging problems is accounting for intraoperative tissue motion resulting from surgical loading conditions. Due to the considerable expense and cumbersome nature of intraoperative MR/CT scanners and the lack of high spatial definition of intracranial anatomy with ultrasound, we have elected to pursue a physics-based computational approach to account for tissue deformation in the context of frameless stereotactic neurosurgery. We have developed a computational model of the brain based on porous media physics and have begun to quantify subsurface deformation due to comparable surgical loads using an *in vivo* porcine model. Templates of CT-observable markers are implanted in a grid-like fashion in the pig brain to quantify tissue motion. Preliminary results based on the simplest of model assumptions are encouraging and have predicted displacement within 15% of measured values. In this paper, a series of computations is compared to experimental data to further understand the impact of material properties and pressure gradients within a homogenous model of brain deformation. The results show that the best fits are obtained with Young's moduli and Poisson's ratio which are smaller than those values typically reported in the literature. As the Poisson ratio decreases towards 0.4 the corresponding Young's modulus increases towards the low end of the values contained in the literature. The optimal pressure gradient is found to be within physiological limits but generally higher than literature values would suggest for a given level of imparted loading, although differences between our experiments and those in the literature with respect to tissue loading conditions are noted.

Key Words: stereotactic neurosurgery, subsurface brain deformation model, brain material properties

1. INTRODUCTION

In recent years, imaging technology has allowed the coregistration of surgical instrument spatial location with preoperative images obtained from modalities such as CT and MR. In the context of neurosurgery, the capability of registering OR and image spaces has provided the possibility of performing stereotactic tasks without the need for a frame attached to the cranium[1-6]. Further, the ability to track instrument location relative to patient-specific anatomical landmarks visible through volumetric image information offers navigational assistance to the neurosurgeon that leads to procedures which are safer, more precise and less invasive. However, because the coregistration is based on preoperative data, brain shift which occurs intraoperatively is not considered but has the potential to produce inaccuracies that could invalidate the frameless stereotactic approach. In previous studies, we have shown that the average shift of the cortical surface of the brain during various neurosurgical procedures is 1 cm with a definite predisposition of the brain surface to move in the direction of gravity[7]. Dickhaus et al. quantified brain shift specifically for tumor resections by tracking brain structures using MR pre- and intraoperatively. They found that surface motion was on the order of 2 cm, and subsurface shift was 6 to 7 mm for positions located at the

[0]For further information contact: keith.paulsen@dartmouth.edu, 8000 Cummings Hall, Hanover, N.H. 03755, Office: 603-646-2695 , Fax: 603-646-3856.

interhemisphere fissure and the lateral ventricles[8]. These studies highlight the fact that centimeter-scale motion routinely occurs during neurosurgery suggesting that intraoperative brain shift cannot be ignored during frameless stereotactic procedures.

To address this problem, we have adopted a physics-based modeling approach to predict deformation from surgical loads in order to update the neurosurgeon's navigational perspective intraoperatively. Our initial modeling efforts have been based on a biphasic porous media representation of brain tissue in which case we have been able to predict *in vivo* displacements in the porcine brain within an average error of 15% under the simplest of model assumptions[9,10]. Ultimately, we envision that a computational model of brain tissue deformation would be used in conjunction with a limited amount of concurrently obtained operative data (e.g. video-tracked surface movement and subsurface ultrasound) in order to estimate subsurface tissue motion and thereby provide updated anatomical information for improved navigational assistance during frameless stereotaxy procedures.

In previous work[9,10], we have used a homogenous representation of the brain with displacement and pressure boundary conditions to represent comparable surgical loads. Unfortunately, only a modest amount of data on brain tissue mechanical properties has been reported in the literature. Early studies used mechanical devices to measure properties *in vivo* but were semi-quantitative at best[11−15]. A new and exciting area of research has emerged using MR and ultrasound to image transverse strain waves thereby allowing the calculation of regional mechanical properties based on strain measurements[16,17]. While more quantitative tissue property information can be anticipated in the future based on these newer techniques, the current uncertainty in brain tissue mechanical properties has led us to investigate the effect of varying Young's modulus and Poisson's ratio in our simplified homogenous model as well as the pressure gradient which acts as a distributed body force with respect to elastic deformation. The goal is to shed some light on the range of mechanical properties of brain tissue by comparing a series of computations with experimental data. The results show that an optimal Young's modulus exists which varies with Poisson's ratio. The calculations indicate that an optimal pressure gradient for a given Young's modulus and Poisson's ratio also exists.

2. THE COMPUTATIONAL MODEL

Previous literature reflects the existence of two major subcategories of brain tissue modeling. The first results from a substantial effort which appeared in the 1970's and centered around brain injury effects. These models were concerned with brain trauma resulting from impacts during automobile crashes [18−20]. Loading conditions for these studies were large accelerations of the cranium followed by sharp decelerations or impact. An example of a recent study in this area was performed by Ruan et al. and consisted of a 2D axisymmetric plane strain finite element computation incorporating a modest number of elements, an idealized skull and a layered structure of cranial contents[21].

The second major subcategory of brain tissue modeling has resulted in simulations of the brain in the context of pathophysiologies such as hydrocephalus and hemorrhage[22−27]. This work involved a more complex representation of the brain as a multi-phasic porous medium. Prior to our recent developments, these computations were performed only in 2D and demonstrated qualitative promise. We have recently extended this approach contributing the first 3D calculations in the context of modeling brain motion under surgically-induced loading conditions and have provided the first *in vivo* attempts to quantify its 3D predictive potential[10].

The theory underpinning this type of brain tissue model originates from the soil mechanics literature and describes the process of consolidation[28]. Consolidation theory is biphasic in nature where the medium consists of a solid matrix/tissue that is saturated with an incompressible fluid throughout the interstitial spaces. Subject to a deformation source, tissue consolidation results in an instantaneous deformation at the area of contact followed by additional deformation caused from exiting interstitial fluid driven by a pressure gradient. Others have recognized the utility of applying consolidation theory to soft tissue mechanics, including Taylor[29,30] who created an interstitial transport model taking into account plasma protein movement and interstitial swelling. Basser[31] has also used a consolidation approach to model infusion-induced swelling in the brain. Computationally, at least in terms of brain tissue mechanics, the work of Nagashima et al. represents the first and most extensive experience with consolidation in the neuroanatomy context[22−24].

The governing equations we have considered for consolidation in soft-tissue can be written as

$$\nabla \cdot G\nabla \mathbf{u} + \nabla \frac{G}{1-2\nu}(\nabla \cdot \mathbf{u}) - \alpha \nabla p = 0 \tag{1a}$$

$$\alpha \frac{\partial}{\partial t}(\nabla \cdot \mathbf{u}) + \frac{1}{S}\frac{\partial p}{\partial t} - \nabla \cdot k\nabla p = 0 \tag{1b}$$

where,

G is shear modulus,
ν is Poisson's ratio,
$\mathbf{u}$ is the displacement vector,
p is the pore fluid pressure,
α is the ratio of fluid volume extracted to volume change of the tissue under compression,
k is the hydraulic conductivity, and
$1\backslash S$ is the amount of water which can be forced into the tissue under constant volume.

These equations assume that the tissue is linearly elastic and that the interstitial fluid is incompressible. Equation (1a) represents classic static mechanical equilibrium subject to a body force represented by an interstitial fluid pressure gradient across the medium. Equation (1b) provides the constitutive relationship between volumetric strain and fluid pressure. Generally, the brain can be considered as a saturated medium which eliminates the time rate of change in pressure from equation (1b) (i.e. $\alpha = 1$, $1\backslash S = 0$), and we have made this assumption in the results reported herein. Although more complex theories exist for soft tissue modeling[32–35], consolidation seems to be a natural starting point in the development of a brain tissue model. It has an advantage over simple linear elasticity due to the added fluid component; this allows access to more realistic boundary conditions related to intracranial pressure and cerebrospinal fluid (CSF) drainage while still maintaining the computational advantages of a linear theory.

3. METHODS

The equations described in (1a-b) have been solved in three dimensions using the Galerkin finite element method (FEM) and were compared to analytical and numerical benchmarks in the literature which has shown that our computational approach is highly accurate (errors less than 2% of applied load on modest levels of finite element mesh resolution). In addition, we have also performed a stability analysis of the equations to better understand the propagation of numerical errors[36]. We have quantified our preliminary experiences with an *in vivo* porcine model and have found we can predict the total average displacement to within 15% of the maximum imparted measured displacement[10].

The experimental surgical procedure involved implanting a pig brain with small 1mm beads in a grid-like fashion in the parenchyma which serve as tissue displacement markers. Following implantation and evaluation of the marker fixation, a balloon catheter filled with contrast agent was inserted in the cranium. All objects were easily seen in a CT scanner and were monitored during subsequent balloon inflations thus creating deformation maps which can be compared to model calculations. Figure 1 shows an example of a pig cranium during a 1cc inflation of the balloon with the tissue thresholded out and the markers/balloon easily observable. Prior to the surgical procedure, a complete set of MR images were taken of the pig cranium. These scans serve as the basis of the FEM discretization process. Using **ANALYZE Version 7.5 - Biomedical Imaging Resource** (Mayo Foundation, Rochester, M.N.), we segmented the 3D volume of interest and used **MATLAB** (Math Works Inc., Natick Mass.) to render the surface boundary description of the brain and any surgical implants. We then produced a tetrahedral grid on the interior using mesh generation software[37] which completed the discretization process. Figure 2 displays a typical mesh in the 1cc deformed state (i.e. after computation) where volume elements are approximately 1 mm^3 inside the tissue (prior to calculation) and 0.025 mm^3 near the implanted catheter (prior to calculation). The mesh contained 11,923 nodes and 62,439 tetrahedral elements.

4. RESULTS

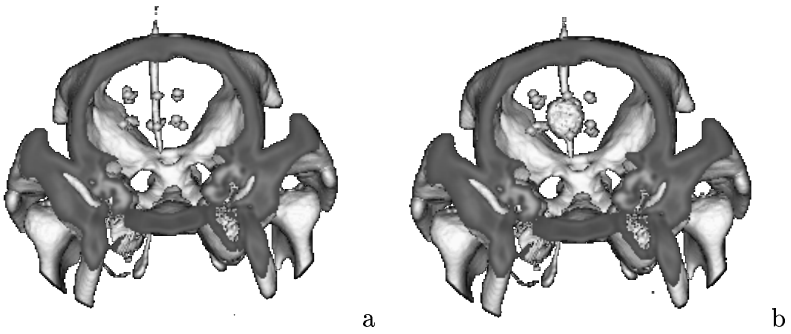

Figure 1. Experimental porcine model with centrally placed balloon catheter, tissue thresholded out, and surrounding grid of 1mm ss markers: (a) baseline volume with uninflated catheter; (b) 1cc inflation with subsequent bead movement.

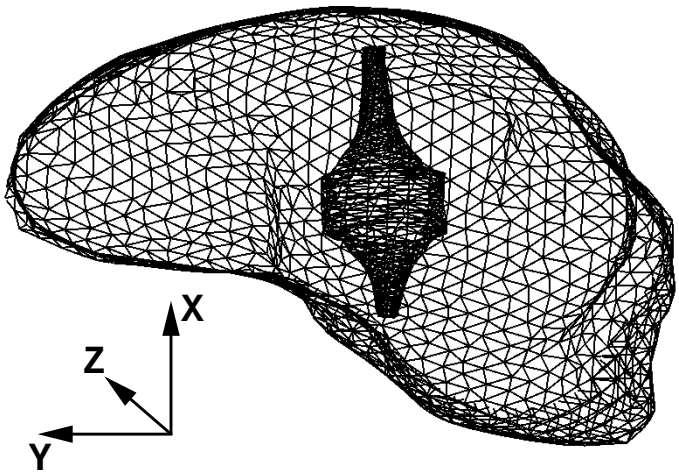

Figure 2. Deformed boundary at the 1cc inflation level.

In previous work[10], we have shown that we are capable of predicting the total average displacement level to within 14% and 19% of the maximum bead displacement over 1cc and 2cc inflation levels, respectively. Figure 2 represents the typical geometries resulting from our calculations. This example was computed using the following properties,

Material Properties: $E = 2100\ Pa$, $\nu = 0.45$, $k = 1e-7\ \frac{m^3 s}{kg}$
Running Properties: $dt = 1e4\ s$, $\theta = 1$, # steps=5.

In terms of boundary conditions, the balloon catheter was divided into two sections which included deformed (cylindrical portion of catheter with 5.45 mm outward expansion) and free surface components (necked portion of catheter). The interstitial pressure at the balloon/tissue interface was taken to be constant at 6000 Pa (or 45 mmHg) which is within the range of values recorded by Wolfla et al.[38,39] under conditions of acute balloon inflation within a closed cranial cavity of the pig. The outer cortical brain surface was prescribed as a fixed (no displacement) boundary with zero fluid pressure.

Starting with the above boundary conditions and varying Young's modulus and Poisson's ratio, we have been able to produce a description of how the average total displacement error varies over the solution domain. Figure 3 represents the average match between the data and calculations for the total displacement of the 15 beads that were tracked in the CT for the 1cc inflation level. It demonstrates that as the solid matrix becomes more incompressible ($\nu \to 0.5$) the minimum error occurs at lower moduli for the homogenous case. Another interesting phenomena is that the convexity of the minimum becomes more pronounced with decreasing Poisson's ratio. From Figure 3, an average total displacement error of 13.8% occurs at a Young's Modulus of 1800 Pa and Poisson's ratio of

0.45. Figure 4 displays the complete comparison between experiment and calculation for each bead displacement directional component as well as the total displacement for these values of Young's modulus and Poisson's ratio.

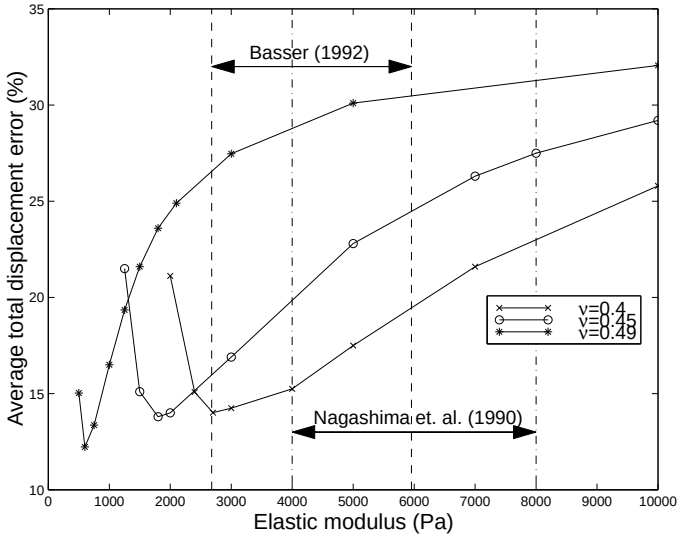

Figure 3. Average match between data and calculation for varying Young's modulus and Poisson's ratio.

In addition to total displacement, the average error in each bead's directional component can be analyzed in a similar fashion to that of Figure 3. These results are shown in Figure 5 and demonstrate that a similar shift in minimum error values is accompanied with increasing Poisson's ratio. Figures 3 and 5 also indicate some brain moduli ranges from the literature where the lower values represent white matter and the upper values correspond to gray matter. The Nagashima et al. and Basser papers used Poisson's ratios used of 0.47 and 0.49 respectively.

We have also quantified how the solution is influenced by the pressure gradient across the tissue which is another important model variable beyond the solid matrix material properties. Figure 6 represents the effect of pressure on each average directional error component as well as the total displacement error. Interestingly, the pressure gradients which correspond to the minimum error in the directional components occur at quite different values. Based on this results, it follows that the minimum total displacement error exists at a gradient value which is a weighting of the different minima that appear in Figure 5. In addition to our calculations, pressure ranges are shown from the Wolfla et al. data which was obtained in a porcine model[38,39]. The 1996 data represents the approximate maximum/minimum interstitial pressure ranges for 1cc-3cc inflation levels of an acute expanding frontal epidural mass (balloon catheter)[38]. The 1997 data represents the pressures associated with the same inflation level range for an acute expanding extradural temporal mass[39].

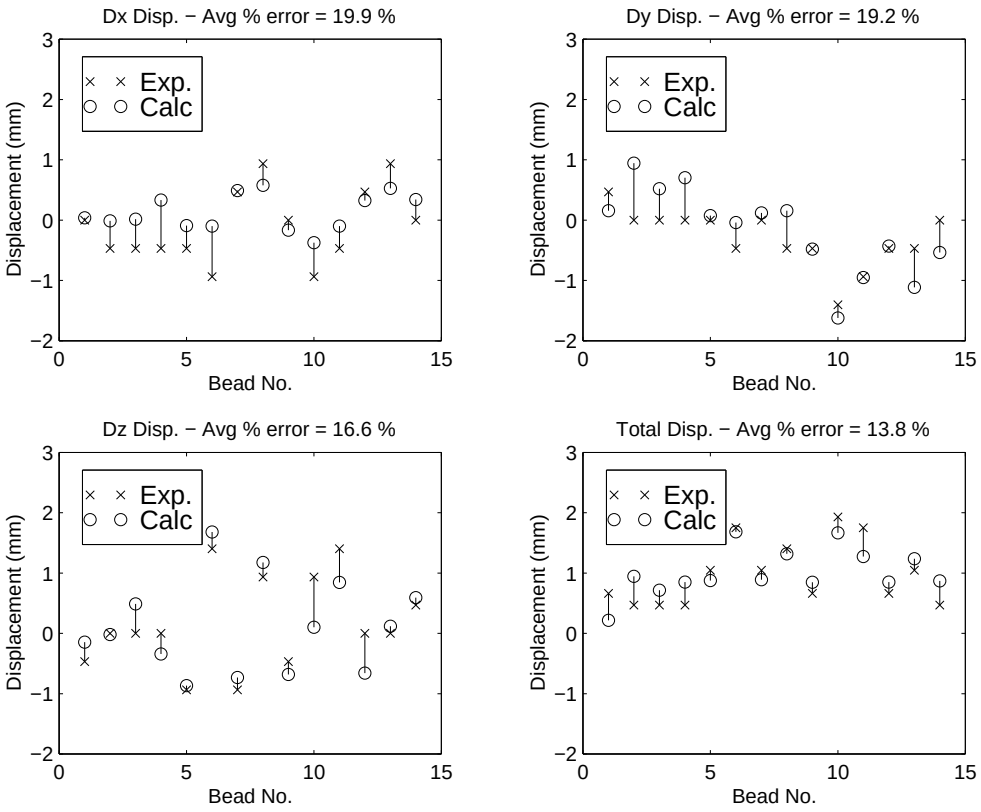

Figure 4. Comparison between measured and calculated data for displacement error at the 1cc inflation level of the balloon catheter.

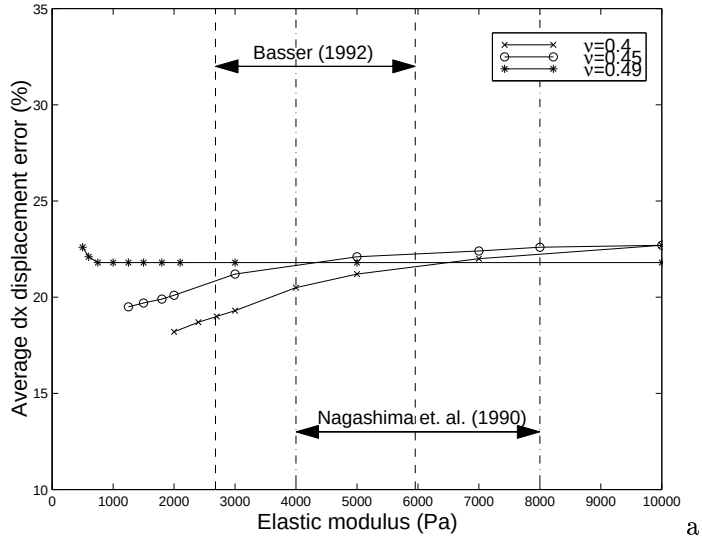

a

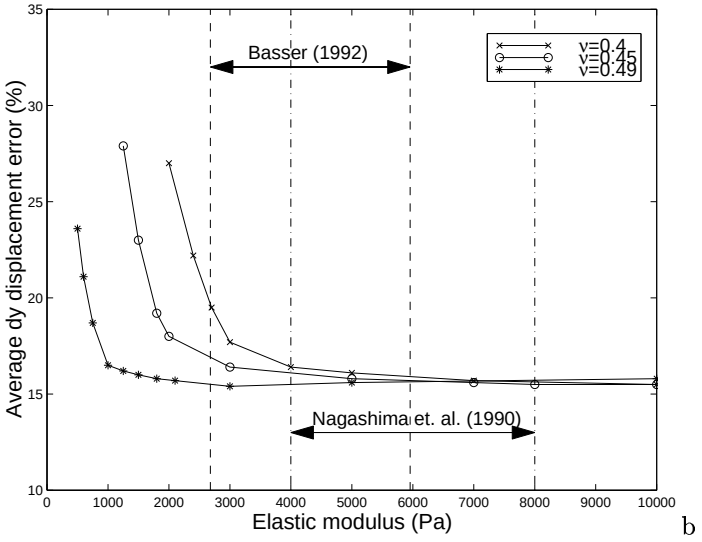

b

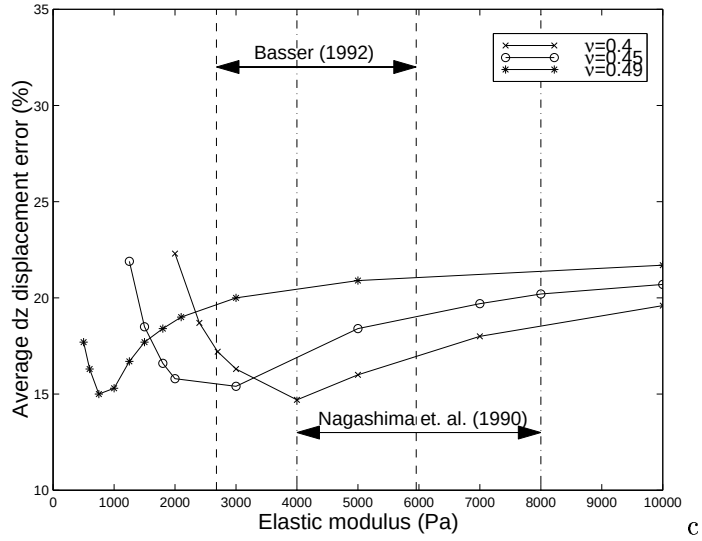

c

Figure 5. Comparison between measured and calculated data for average directional displacement error for 1cc inflation level of balloon catheter for varying Young's modulus and Poisson's ratio.

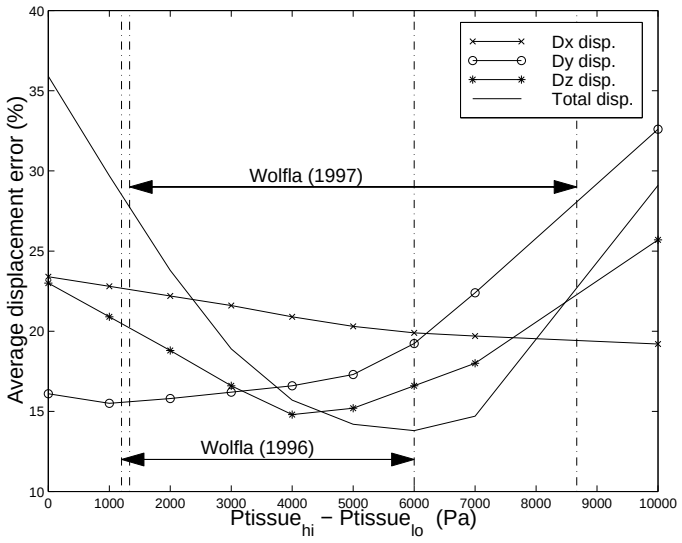

Figure 6. Comparison between measured and calculated data for average displacement error for 1cc inflation level of balloon catheter while varying pressure across the tissue.

5. CONCLUSIONS

We have shown in the case of a homogenous model of brain deformation based on consolidation theory subject to displacement and pressure boundary conditions that minimum average displacement error varies with Young's modulus, Poisson's ratio, and pressure gradient. We have also found that as the solid matrix becomes more incompressible (i.e. $\nu \to 0.5$), the error minimum shifts downward towards a smaller Young's modulus. Typically the literature has considered brain tissue as nearly incompressible. Interestingly, we observe that the ranges of accepted moduli values for brain do not correlate with the typical Poisson's ratio cited (assuming that brain moduli ranges are close in value across species). This is not to say that the incompressible assumptions made in previous studies are incorrect but the results do suggest that further study is required. With respect to the effect of tissue pressure gradients, we find that our optimal gradient falls inside the range of physiological limits. Although the lower values of the Wolfla range (1cc inflation level) are significantly lower than our optimum, it is important to recognize that our balloon placement was intraparenchymal and its effects are not yet quantified. The variation in the upper range for the two different placements in the Wolfla studies suggests that placement could indeed have a substantial effect on the pressure gradients that occur in tissue under acute expansion.

Clearly, one of the major assumptions in these calculations is tissue homogeneity. Effort is currently underway to employ a heterogeneous model to further investigation of the effects of varying moduli and Poisson's ratio in our *in vivo* model. We are also developing more refined techniques for imparting tissue displacement in a more controlled and quantifiable manner. It is the hope that these studies will lay the ground work for a real-time, model-based updating of surgeon's navigational fields in the context of frameless stereotactic neurosurgery.

Acknowledgement: This work was supported by National Institutes of Health grant R01-NS33900 awarded by the National Institute of Neurological Disorders and Stroke. ANALYZE software was provided in collaboration with the Mayo Foundation.

6. REFERENCES

1. T. Peters, B. Davey, P. Munger, R. Comeau, A. Evans, and A. Olivier, 'Three-dimensional multimodal image-guidance for neurosurgery',*IEEE Trans. Med. Imaging*, vol. 15, pp. 121-128, 1996.
2. W. E. L. Grimson, G. J. Ettlinger, S. J. White, T. Lozano-Perez, W. M. Wells 3rd, and R. Kikinis, 'An automated registration method for frameless stereotaxy, image guided surgery and enhanced reality visualization', it IEEE Trans. Med. Imaging, vol. 15, pp. 129-140, 1996.
3. D. W. Roberts, J. W. Strohbehn, J. F. Hatch, W. Murray, and H. Kettenberger, ' A frameless stereotactic integration of computerized tomographic imaging and the operating microscope', *J. Neurosurg.*, vol. 65, pp. 545-549, 1986.
4. R. L. Galloway, R. J. Maciunas, and C. A. Edwards, 'Interactive image-guided neurosurgery', *IEEE Trans. Biomed. Eng.*, vol. 39, pp. 1226-1231, 1992.
5. G. H. Barnette, D. W. Kormos, and C. P. Steiner, 'Use of a frameless, armless stereotactic wand for brain tumor localization with 2D and 3D neuroimaging', *Neurosurgery*, vol. 33, pp. 674-678, 1993.
6. D. R. Sanderman, and S. S. Gill, 'The impact of interactive image guided surgery: the Bristol experience with the ISF/Elekta viewing wand', *Acta Neurochirurgica, Suppl.*, vol. 64, pp. 54-58, 1995.
7. D. W. Roberts, A. Hartov, F.E. Kennedy, M. I. Miga, K. D. Paulsen, 'Intraoperative brain shift and deformation: a quantitative clinical analysis of cortical displacements in 28 cases', *Neurosurgery*, (submitted), 1997.
8. H. Dickhaus, K. Ganser, A. Staubert, M. M. Bonsanto, C. R. Wirtz, V. M. Tronnier, and S. Kunze, 'Quantification of brain shift effects by mr-imaging', *Proc. An. Int. Conf. IEEE Eng. Med. Biology Soc.*, 1997.
9. M. I. Miga, K. D. Paulsen, F. E. Kennedy, P. J. Hoopes, A. Hartov, and D. W. Roberts, 'A 3D brain deformation model experiencing comparable surgical loads', *Proc. 19th An. Int. Conf. IEEE Eng. Med. Biology Soc.*, 773-776, 1997.
10. K. D. Paulsen, M. I. Miga, F. E. Kennedy, P. J. Hoopes, A. Hartov, and D. W. Roberts, 'A computational model for tracking subsurface tissue deformation during stereotactic neurosurgery', *IEEE Transactions on Biomedical Engineering*, (submitted), (1997).
11. G. T. Fallenstein, and V. D. Huke, 'Dynamic mechanical properties of brain tissue', *J. Biomech.*, vol. 2, pp. 217-226, 1969.
12. C. Ljung, 'A model for brain deformation due to rotation of the skull', *J. Biomechanics*, vol. 8, pp. 263-274, 1975.
13. E. K. Walsh, and A. Schettini, 'A pressure-displacement transducer for measuring brain tissue properties in vivo', *J. Appl. Physiol.*, 38, 187-189, (1975).
14. E. K. Walsh, W. Furniss and A. Schettini, 'On measurement of brain elastic response in vivo', *Am. J. Physiol.*, vol. 232, pp. R27-R30, 1977.
15. E. K. Walsh, and A. Schettini, 'Calculation of brain elastic parameters in vivo', *Am. J. Physiol.*, 247, R693-R700, (1984).
16. R. Mathupillai, P. J. Rossman, D. J. Lomas, J. F. Greenleaf, S. J. Riederer, and R. L. Ehman, 'Magnetic resonance elastography by direct visualization of propagating acoustic strain waves', *Science*, vol. 269, pp. 1854-1857, (1995).
17. R. Mathupillai, P. J. Rossman, D. J. Lomas, J. F. Greenleaf, S. J. Riederer, and R. L. Ehman, 'Magnetic Resonance Imaging of Transverse Strain Waves', *Magnetic Resonance in Medicine*, vol. 36, pp. 266-274, (1996).
18. T. A. Shugar, and M. G. Katona, 'Development of a finite element head injury model', *ASCE J. Eng. Mech. Div.*, EM3:101, E173, pp. 223-239, 1975.

19. C. C. Ward, and R. B. Thompson, 'The development of a detailed finite element brain model', *Proc. 19th Stapp Car Crash Conf.*, pp. 641-674, 1975.

20. T. B. Khalil, and R. P. Hubbard, 'Parametric study of head response by finite element modeling',*J. Biomech*, vol. 10, pp. 119-132, 1977.

21. J. A. Ruan, T. B. Khalil, and A. I. King, 'Human head dynamic response to side impact by finite element modeling', *ASME J. Biomech. Eng.*, vol. 113, pp. 276-283, 1991.

22. T. Nagashima, T. Shirakuni, and SI. Rapoport, 'A two-dimensional, finite element analysis of vasogenic brain edema,' *Neurol. Med. Chir.*, vol. 30, pp. 1-9, 1990.

23. T. Nagashima, Y. Tada, S. Hamano, M. Skakakura, K. Masaoka, N. Tamaki, and S. Matsumoto, 'The finite element analysis of brain oedema associated with intracranial meningiomas', *Acta. Neurochir. Suppl.*, vol. 51, pp. 155-7, 1990.

24. T. Nagashima, N. Tamaki, M. Takada, and Y. Tada, 'Formation and resolution of brain edema associated with brain tumors. A comprehensive theoretical model and clinical analysis', *Acta Neurochir Suppl*, vol. 60, pp. 165-167, 1994.

25. Y. Tada, and T. Nagashima, 'Modeling and simulation of brain lesions by the finite-element method', *IEEE Eng. Med. Bio.*, pp. 497-503, 1994.

26. H. Takizawa, K. Sugiura, M. Baba, C. Kudou, S. Endo, M. Nakabayashi, and R. Fukuya, 'Deformation of brain and stress distribution caused by putaminal hemorrhage–numerical computer simulation by finite element method', *No To Shinkei*, vol. 43, pp. 1035-1039, 1991.

27. H. Takizawa, K. Sugiura, M. Baba, and J. D. Miller, 'Analysis of intracerebral hematoma shapes by numerical computer simulation using the finite element method', *Neurol Med Chir*, vol. 34, pp. 65-69, 1994.

28. M. Biot, 'General theory of three dimensional consolidation', *J. Appl. Phys.*, vol. 12, pp. 155-164, 1941.

29. D.G. Taylor, J.L. Bert, and B.D. Bowen, 'A mathematical model of interstitial transport. I. Theory', *Microvasc Res*, vol. 39, pp. 253-278, 1990.

30. D.G. Taylor, J.L. Bert, and B.D. Bowen, 'A mathematical model of interstitial transport. II. Microvasculature exchange in the mesentery', *Microvasc Res*, vol. 39, pp. 279-306, 1990.

31. P. J. Basser, 'Interstitial pressure, volume, and flow during infusion into brain tissue', *Microvasc. Res.*, vol. 44, pp. 143-165, 1992.

32. K. K. Mendis, R. L. Stalnaker, and S. H. Advani, 'A constitutive relationship for large deformation finite element modeling of brain tissue', *J Biomech Eng*, vol. 117, pp. 279-285, 1995.

33. R. L. Spilker, and J. K. Suh. 'Formulation and evaluation of a finite element model for the biphasic model of hydrated soft tissue', *Comp. Struct.*, vol. 35, no. 4, pp. 425-439, 1990.

34. R. L. Spilker, and T. A. Maxian. 'A mixed-penalty finite element formulation of the linear biphasic theory for soft tissues', *Int. J. Numer. Methods Eng.*, vol. 30, pp. 1063-1082, 1990.

35. J.P. Laible, D. Pflaster, B. R. Simon, M. H. Krag, M. Pope, and L. D. Haugh, 'A dynamic material parameter estimation procedure for soft tissue using a poroelastic finite element model', *J Biomech Eng*, vol. 116, pp. 19-29, 1994.

36. M. I. Miga, K. D. Paulsen, F. E. Kennedy, 'Von Neumann stability analysis of Biot's general two-dimensional theory of consolidation', *Int. J. of Num. Methods in Eng.*, (submitted), (1997).

37. J. M. Sullivan Jr., G. Charron, and K. D. Paulsen, 'A three dimensional mesh generator for arbitrary multiple material domains, *Finite Element Analysis and Design*, vol. 25, pp. 219-241, 1997.

38. C. E. Wolfla, T. G. Luerssen, R. M. Bowman, and T. K. Putty, 'Brain tissue pressure gradients created by expanding frontal epidural mass lesion', *J. Neurosurg.*, vol. 84, pp. 642-647, 1996.

39. C. E. Wolfla, T. G. Luerssen, and R. M. Bowman, 'Regional brain tissue pressure gradients created by expanding extradural temporal mass legion', *J. Neurosurg*, vol. 86, pp. 505-510, 1997.